New Mixed Compound $Cs_{2.8}Tl_{1.2}(SO_4)_{1.48}(SeO_4)_{0.52}.[Te(OH)_6]_2$: Synthesis, Structural Characterization, Vibrational Studies and Phase Transitions

Fatma Ben Tahar [a], Atef Elferjani [a *], Santiago Garcia-Granda [b], Mohamed Dammak [a].

[a] *Laboratory of Inorganic Chemistry, LR 17ES07, University of Sfax, B. P. 1171, Sfax 3000, Tunisia.*

[b] *Department of Physical and Analytical Chemistry, University Oviedo-CINN, 33006 Oviedo, Spain.*

*E-mail address: elferjani.atef@yahoo.fr

Abstract

The new compound $Cs_{2.8}Tl_{1.2}(SO_4)_{1.48}(SeO_4)_{0.52}.[Te(OH)_6]_2$ (CsTlSSTe) was characterized by X-ray single crystal analysis performed at room temperature, revealing that it crystallizes in the space group $P2_1/n$, with the following crystal data: a= 11.8967(4)Å, b= 14.1486(5) Å, c= 13.1612(5) Å, β= 108.973(1)°, V= 2094.96(13) $Å^3$ and Z = 4. However, the main features of these atomic arrangements consist in the coexistence of three different anions in the unit cell, connected by (O–H…O) hydrogen bonds that pave the way for building the crystal. Furthermore, the spectroscopic results, at room temperature, confirmed the existence of both cationic and anionic parts, which is in perfect harmony with the results obtained from structural measurements. Three-phase transitions at (411, 425 and 498) K were obtained by means of Differential scanning calorimetry (DSC). Finally, thermal decomposition of the sample salt takes place at much higher temperatures, with an onset of approximately 437 K.

Key words: Crystal structure; Thermal analysis; Phase transitions; Vibrational study.

1. Introduction

The deep interest in various inorganic compounds originates from hydrogen-bonded telluric acids concerning the well-established applications, as these will determine their potential applications such as electrochemical reactors, solid-state batteries and multilayer capacitors [1]. Remarkably, telluric acid is capable of forming stable adduct together with some varieties of inorganic materials, as sulfates and selenates, hence acting as both acceptor and donor of hydrogen bonds [2–4]

The tellurate family belongs to a very important class of compounds with the general formula $M_2AO_4Te(OH)_6$ (where M is a monovalent cation: Na^+, K^+, NH_4^+, Tl^+, Rb^+ and Cs^+, X = S, Se and HP) [5–10]. So far, the most important structural property of these crystals is the presence of some anionic groups (TeO_6^{6-} , SO_4^{2-} and SeO_4^{2-}) in the unit cell. Overall, another key feature of these compounds pertains to the hydrogen bonds, formed in their crystal structure, which represents further evidence for the significance of such family [11–16].

The anionic substitution has already been explored from the structural arrangements perspective. In fact, tellurates, caesium sulfate selenate tellurate, $Cs_2(SO_4)_{0.57}(SeO_4)_{0.43}.Te(OH)_6$ (CsSSeTe) [11], thallium sulfate selenate tellurate, $Tl_2(SO_4)_{0.61}(SeO_4)_{0.39}.Te(OH)_6$ (TlSSeTe) [12] represent some of these compounds that are recognized by centrosymmetry and crystallization in the monoclinic system with $P2_1/c$ space group. Yet, in the original compound, caesium sulfate tellurate (CsSTe) undergoes a ferroelectric–paraelectric phase transition at T = 490 K and a superprotonic one at 500 K [10].

What is worthwhile to note is that these are structural transitions in terms of discovering physical properties, including ferroelectricity and superionic-protonic conduction, referring principally to the motion of the proton H^+ via the hydrogen bonds [1, 5, 10, 14–16].

The present paper undertakes the study of the effect of the simultaneous cationic and anionic substitution on the structural properties. Actually, it reports the synthesis, the structural characterization by X-ray diffraction, vibrational studies and thermal analysis of the mixed crystal $Cs_{2.8}Tl_{1.2}(SO_4)_{1.48}(SeO_4)_{0.52}.[Te(OH)_6]_2$ (CsTlSSeTe).

2. Experimental Section

2.1. Synthesis

The crystal of the formula $Cs_{2.8}Tl_{1.2}(SO_4)_{1.48}(SeO_4)_{0.52}.[Te(OH)_6]_2$ was synthesized by slow evaporation, at room temperature, from aqueous solution containing telluric acid H_6TeO_6, cesium carbonate Cs_2CO_3, thallium carbonate Tl_2CO_3, sulfuric acid H_2SO_4 and selenic acid H_2SeO_4 repeated in the stoechiometric ratio. Schematically the reaction is:

$$(1\text{-}y)\ Cs_2CO_3 + y\ Tl_2CO_3 + (1\text{-}x)\ (H_2SO_4) + x\ H_2SeO_4 + 2H_6TeO_6 \rightarrow$$

$$Cs_{2\text{-}2y}Tl_{2y}(SO_4)_{1\text{-}x}(SeO_4)_x[Te(OH)_6]_2 + CO_2 + H_2O \qquad (1)$$

After approximately 14 days of evaporation, the pure, colorless and transparent crystals of sharp contours were obtained. The obtained single crystal suitable for X-ray diffraction analysis was selected and studied. The different atoms were chemically analyzed to confirm the formula determined by structural refinement.

2.2. Crystal data and structure determination

A CsTlSSeTe crystal was selected in order to carry out the structural study by X-ray diffraction. Single-crystal X-ray data were carefully selected under a polarizing microscope and glued to a cactus needle mounted on a four-circle Bruker Kappa Apex II CCD area detector diffractometer equipped with graphite monochromatic MoKa radiation (k= 0.71073 Å) for data collection at room temperature [17, 18]. Lorentz and polarizing effect corrections were performed before proceeding to the refinement of the structure.

For unit cell refinement, a total of reflection collected with θ ranging from 2.8 to 26.8 of which 2982 have $I > 2\sigma(I)$ and were used for structure determination. At room temperature, refinements were carried out using the crystallographic CRYSTALS program [19] in the monoclinic system with $P2_1/n$ space group (Z= 4). Moreover, the refinement of Te, Tl and Cs atoms was conducted using Patterson methods, while the non-hydrogen atoms that remained were obtained from the successive difference Fourier maps via SHELXL-97 program [20]. All hydrogen atoms are placed geometrically. After successive refinements based on F^2, we obtained a reliability factor *R* of 0.056 and the structure of graphics are created with the Diamond program [21].

Correspondingly, the pertinent experimental details of the structure determination, data collection and refinements for the new (CsTlSSeTe) compound are presented in Table S1 in the Supporting Information. Furthermore, Tables S2 and S3 illustrate the final atomic positions and the U_{eq} parameters and the anisotropic displacement parameters. Besides, the

main interatomic distances (Å) and bond angles (°) for our solid solution are summarized in Table 1.

2.3. Spectroscopic measurements

Spectroscopic studies were undertaken for the quantification of the new crystal. Using a Jasco-FT-IR-420 spectrophotometer, the infrared spectrum of the CsTlSSeTe was recorded at room temperature in the wave number range between 400 and 4000 cm^{-1} with a sample pressed in a KBr pellet. Moreover, the Raman spectrum was performed at room temperature between 50 and 1200 cm^{-1} using a single monochromatic spectrophotometer notch filter on a Labrama HR 800 instrument.

2.4. Thermal studies

The differential scanning calorimetry measurements were performed on a SETARAM apparatus, with the samples (about 4.966 mg) in aluminum crucibles under a nitrogen atmosphere with heating rate of 5 K/min from 340 to 550 K.

For the thermogravimetry and differential thermal analysis, the (TG-DTA) analysis was investigated on a Mettler Toledo model TGA851ELF and Setaram model Setsys Evolution 16 thermobalances, by heating the sample in an aluminum crucible between 340 and 600 K under air at a heating rate of 10 K min^{-1}. The 15.833 mg powdered sample was used in the TG and DTA measurements.

3. Results and discussion

3.1. Structural Study

Fig. 1a. presents the crystal structure of $Cs_{2.8}Tl_{1.2}(SO_4)_{1.48}(SeO_4)_{0.52}.[Te(OH)_6]_2$ (CsTlSSeTe) in the (001) plane. The title compound belongs to the monoclinic system with $P2_1/n$ space group at room temperature, and the unit cell parameters are: a= 11.8967(4) Å, b= 14.1486(5) Å, c= 13.1612(5) Å, β= 108.973(1)°, Z = 4 and V= 2097.96(13) $Å^3$.

Fig. 1a. shows that the structure can be regarded as being built up by (TeO_6^{6-}, SO_4^{2-} and SeO_4^{2-}) groups, alternating with the (Cs^+/Tl^+) cations, connected by O–H…O hydrogen bonds. Its structure can be regarded as being built by planes of pure $Te(OH)_6$ (at x = 0 and x = a/2) octahedra, alternating with planes of pure SO_4/SeO_4 (at x = a/4 and x = 3a/4) tetrahedra. Between these kinds of polyhedra are situated the Cs^+ and Tl^+ cations.

In the novel CsTlSSeTe structure, the tellurium atom occupies one general position and two specific ones, which indicates that our structure displays three types of octahedrons: $Te(1)O_6$,

$Te(2)O_6$ and $Te(3)O_6$ (Fig. 1b.). The main distances Te–O and bond angles for these octahedra are presented in Table 1, and TeO_6 groups in Fig. 1b. In Fact, the minimum and maximum Te–O distances in TeO_6 octahedra are 1.848 (1) and 1.926(1) Å and O–Te–O angles between 88.0(4) and 92.6(5)° . From the values already shown in Table 1, it can be observed that these TeO_6 in the novel mixed solid solution are less deformed if compared with the octadedrons in previously studied compounds. Actually, the Te–O distances the CsSSeTe vary from 1.896(8) to 1.937(8) Å with O–Te–O angles between 86.5(4)° and 92.2(4)° [11].

The difference between these Te–O distances and the angular distortion evidently demonstrates that TeO_6 octahedrons are more regular in the new material compared to the CsSSeTe material. Thus, the phenomenon can be ascribed to the existence of various anionic and cationic entities in this compound.

For the S/SeO_4 groups for the new structure CsTlSSeTe, the S/Se atoms are coordinated by four oxygen atoms. Therefore, the new structure displays two types of tetrahedrons, i.e. $S/Se(1)O_4$ and $S/Se(2)O_4$ as illustrated in Fig. 1c. However, in the TlSSeTe and CsSSeTe structures, one type of tetrahedron is presented.

In addition, the S/Se−O distances in the mixed CsTlSSeTe structure vary between 1.466(1) and 1.506(1) Å with O−S/Se−O angles, ranging between 105.9(6)° and 112.5(6)°. These values confirm the distortion of the tetrahedron S/SeO_4 (Table 1).

However, the S/Se–O distances vary from 1.512(9) to 1.562(9) Å for (TlSSeTe) structure [12]. In fact, the distances and angles related to the two tetrahedrons are listed in Table 1.

According to the difference between these values in our structure, the TlSSeTe material is associated with the size of the cation radii, probably accredited to the partial cationic and anionic substitutions.

In the unit cell, the two ions, cesium and thallium occupy general positions between those S/SeO_4 and TeO_6 groups. With reference to Table 1, four types of cations are present, i.e. Cs(1)/Tl(1), Cs(2)/Tl(2), Cs(3)/Tl(3), and Cs(4)/Tl(4).

In this case, eight atoms coordinate the Cs(1)/Tl(1) and Cs(2)/Tl(2) cations in the studied CsTlSSeTe structure (also see Supporting Information, Fig. S1.). Indeed, the environment of Cs(1)/Tl(1) cation is composed of two oxygen atoms (O(4) and O(5)) belonging to $Te(1)O_6$, only one belonging to $Te(2)O_6$ octahedron and two corresponding to the third $Te(3)O_6$ octahedron, one oxygen atom belonging to $S/Se(1)O_4$ tetrahedron, two belonging to the second $S/Se(2)O_4$. The Cs(1)/Tl(1)–O distances range between 2.90(1) Å and 3.276 (9) Å.

The environment of Cs(2)/Tl(2) is formed by three oxygen atoms corresponding to $Te(1)O_6$,

two belonging to the second octahedron $Te(1)O_6$ and only one of them belonging to the third octahedron, while two of them belonging to the S/SeO_4 tetrahedron (Fig. S1.), with Cs(2)/Tl(2) distances varying from 3.03(1) to 3.439(9) Å.

Nevertheless, with respect to the cations in the CsTlSSeTe structure, the Cs(3)/Tl(3) cation is coordinated by 6 oxygen atoms and the Cs(4)/Tl(4) by 7 oxygen atoms. Indeed, the first cation Cs(3)/Tl(3) is coordinated by two oxygen atoms belonging to $Te(1)O_6$, O(8) and O(11) corresponding to $Te(2)O_6$ and $Te(3)O_6$, respectively, and two of them belonging to different tetrahedrons, with Cs(3)/Tl(3)–O distances varying from 3.01(1) to 3.221(9) Å.

On the other hand, the environment of the second cation Cs(4)/Tl(4) is composed of two oxygen atoms belonging to $Te(1)O_6$, one oxygen atom of the second octahedron $Te(2)O_6$, O(12) of the third octahedron $Te(2)O_6$ and the others (O(14), O(16) and O(17)) belonging to $S/Se(1)O_4$ and $S/Se(2)O_4$ tetrahedra (Fig. S1.). The Cs(4)/Tl(4)−O bonds distances are situated between 3.05(1) and 3.49(1) Å. The cesium/thallium coordination is shown in Fig. S1. and their distances are summarized in Table 1.

Therefore, the high coordination and the different types of the cesium and thallium cations in the new CsTlSSeTe account for the stability of this atomic arrangement due to the highly considerable interaction between anionic and cationic groups.

A projection view of the title compound indicating the hydrogen bonding in CsTlSSeTe is presented in Fig. 2. In fact, the S/SeO_4 tetrahedron with the octahedral parts are connected by O−H…O hydrogen bonds laying essentially in the a,c plane (Fig. 2.). The main geometrical features of the hydrogen bonding network are given in Table 2.

By examining this structure, five hydrogen atoms contribute in the formation of the hydrogen bonds (Table 2; Fig. 2.). Thus, the two hydrogen atoms H(1) of the octahedral groups $Te(1)O_6$ are connected to two oxygen atoms O(14) and O(15) of the S/SeO_4 tetrahedral groups. Indeed, the two hydrogen atoms H(2) of the second $Te(2)O_6$ octahedral groups are linked to the two oxygen atoms O(19) and O(20) of the tetrahedral groups . Besides, the two hydrogen atoms H(10) in the third $Te(3)O_6$ octahedral groups are connected to two oxygen atoms of the tetrahedral groups. However, each of the other two hydrogen atoms H(7) and H(8), belonging to the group $T(2)O_6$, are bound to oxygen O (17) and O (19), respectively, of the second $S/Se(2)O_4$ tetrahedron (Fig. 2.).

Furthermore, the O…O distance ranges from 2.646(4) to 3.527(5) Å. Based on the NOVAK criterion [23], those values confirm that the hydrogen bonds are of two types as follows: when the O…O are smaller than 2.7 Å, the bonds are strong, while in the other case, the hydrogen

bonds are weak [23]. Moreover, the O…H distances in this material vary from 1.951 to 2.585 Å and the values of O−H…O angles range between 127.5(7) and 167.4(6)°.

3.2. Vibrational analysis

The crystal structure of the new compound can be easily verified by studying Infrared and Raman spectra at room temperature, which are compared to those found in previous studies about numerous tellurates compounds [1, 15, 16, 24, 25]. In fact, the IR and Raman spectra of CsTlSSeTe, recorded for the wavenumber region between (400–4000) and (50–1200) cm^{-1}, are presented in Figs. S2 and S3. Besides, the wavenumbers of the assignments are shown in Table 3.

3.2.1. Interpretation of IR spectrum

At room temperature, the absorption of $Cs_{2.8}Tl_{1.2}(SO_4)_{1.48}(SeO_4)_{0.52}.[Te(OH)_6]_2$ compound exhibits a symmetry space group $P2_1/n$ with four formula units. It is noteworthy to note that the obtained results pertaining to the TeO_6, SO_4, SeO_4 bands (in Table 3) are in accordance with those obtained in the literature corresponding to the new compound [1, 5, 16, 24–29].

As for the TeO_6 octahedral group, the intense peak located around 673 cm^{-1} is attributed to the symmetric stretching vibration v_1 of (TeO_6), whereas the asymmetric stretching of $v_3(TeO_6)$ is found at the wavenumber 596 cm^{-1} [1, 15, 24, 25].

In addition, all the vibration modes in the SO_4 tetrahedral group are Raman active, while only v_2 and v_3 are IR active. The very weak band detected at 471 cm^{-1} is assigned to v_2 (SO_4) [25, 25], while the band associated with the asymmetric stretching vibration v_3 of (SO_4) appears in the spectra at 1077 cm^{-1} [15, 25–29].

Moreover, the SeO_4 tetrahedral group has all the vibration modes, which are Raman active, whereas only the asymmetric stretching vibration (v_3) mode of (SeO_4) is IR active. Hence, the detected peak appears at 865 cm^{-1} [1, 15, 25, 26].

In the high-frequency region (1300–2600) cm^{-1}, the broad bands at 1481, 2327 and 2365 cm^{-1} in IR can be assigned to the asymmetric as well as the symmetric stretching vibrations of the O−H…O groups of the hydrogen bond, respectively, with respect to this material [25, 29].

Finally, the strong band detected at 3058 cm^{-1} is attributed to the O–H stretching vibration [1, 15, 25].

3.2.2. Interpretation of Raman spectrum

The Raman spectra of both internal and external vibrations pertaining to polycrystalline samples of the new $Cs_{2.8}Tl_{1.2}(SO_4)_{1.48}(SeO_4)_{0.52}.[Te(OH)_6]_2$ (CsTlSSeTe) were registered, at room temperature, between 50 and 1200 cm^{-1} (Fig. S3). In fact, the intense peak around 650 cm^{-1} corresponds to the symmetric stretching $\nu_1(TeO_6)$ [2, 12, 15]. This vibration is detected in the IR spectra at 965 cm^{-1}. The two vibration modes $\nu_4(TeO_6)$ and $\nu_5(TeO_6)$ are noted as two bands at 356 and 362 cm^{-1}, respectively, however, they are not observed in IR spectrum [15, 25, 29].

In addition, the symmetric stretching mode $\nu_1(SO_4)$ appears at the 969 cm^{-1} [2, 14, 16]. The peak, appearing at 475 cm^{-1} in both Raman, is related to the symmetric deformation $\nu_2(SO_4)$ [1, 28, 29], thus being in excellent agreement with the results of the TlKSSeTe and TlNSSeTe compounds [15, 25].

The vibrational modes of the SeO_4 were attributed according to the literature. In fact, the symmetric stretching vibration ν_1 of (SeO_4) occurs at 831 cm^{-1} [1, 15]. However, the two peaks attributed to the $\nu_2(SeO_4)$ and $\nu_4(SeO_4)$ at 319 cm^{-1} and 412 cm^{-1}, respectively, were previously described for several selenates compounds [15].

In the low-frequency region of the spectra (<200 cm^{-1}), the obtained Raman lines, most probably corresponding to the translation modes of Tl^+ cations, occur at 60 cm^{-1} [1, 15, 25], while the very weak line observed under 184 cm^{-1} is assigned to the lattice modes [25].

The band observed under 119 cm^{-1} can be ascribed to the vibration and translation modes of (S/SeO_4^{2-} and TeO_6^{6-}) anions [1, 24]. In the present work, our assignment agrees well with the previous results of Elferjani et al. [1, 15, 25].

3.3 Thermal Analysis

3.3.1. Calorimetry study

A typical result of the calorimetric study of the CsTlSSeTe compound was carried out within the range of 340 to 550 K, which reveals three distinct endothermic peaks detected at 411, 425 and 498 K (Fig. 3a). In fact, the obtained value of the calculated transition enthalpies for the first and second transitions is $\Delta H_1 = 13.81 Jg^{-1}$. However, the third phase transition is $\Delta H_2 = 103.24\ Jg^{-1}$, respectively.

Furthermore, these peaks refer to three-phase transitions. In fact, the first peak corresponds to a structural phase transition [1, 12, 15] and the second one corresponds to the ferro-paraelectric phase transition [1, 15, 24, 29]. Moreover, the third one is intense and exhibits the characteristics of a protonic conduction phase transition [1, 15, 24, 30]. Based on the similar

result, the protonic conduction at high temperature may be elucidated by the breaking of O−H…O hydrogen bonds that connect TeO_6 to S/SeO_4.

3.3.2. Thermogravimetric (TG) and Differential Thermal Analysis (DTA)

DTA and DTG measurements were carried out to highlight the phase transitions observed by DSC study and the thermal stability of the CsTlSSeTe crystal. An overview of the results clearly presents three peaks in the DTA diagram of this material, the presence of three endothermic peaks observed at 417, 420 and 483 K of this material, while the existence of only one mass loss in the TG curve. This compound seems to be stable up to 433 K. Above this temperature, a gradual weight loss appears from 437 K to around 587 K, which is considered as a limit of the thermal stability of the compound (Fig. 3b.).

The endothermic peak observed at 483 K in the DTA thermogram accompanied by a highly considerable weight loss that tends towards 6.43% in the TGA thermogram corresponds to the loss of four water molecules per chemical formula. With reference to the literature [1, 15], this result is in line with the degradation phenomenon of telluric acid which decomposes to disengage the four water molecules, thus yielding the ortho-telluric acid H_2TeO_4 [1, 25] as follows:

$$Cs_{2.8}Tl_{1.2}(SO_4)_{1.48}(SeO_4)_{0.52}.[Te(OH)_6]_2 \longrightarrow Cs_{2.8}Tl_{1.2}(SO_4)_{1.48}(SeO_4)_{0.52}.[H_2TeO_4]_2 + 4H_2O \quad (2)$$

4. Conclusion

In this research work, the effect pertaining to the influence of the simultaneous cationic and anionic substitution on the new material with the general formula ($Cs_{2.8}Tl_{1.2}(SO_4)_{1.48}(SeO_4)_{0.52}.[Te(OH)_6]_2$) is examined and then prepared by slow evaporation from aqueous solution, at room temperature. Furthermore, its crystal structure is determined by means of single-crystal XRD.

The new solid solution crystallizes in the monoclinic system ($P2_1/n$ space group) at room temperature. The structure can be regarded as being built of planes of TeO_6 octahedron and pure S/SeO_4 tetrahedron, with Cs^+ and Tl^+ cations intercalating between these planes. The crystal packing of the title material is stabilized by rich O−H…O hydrogen bonds.

Indeed, the Infrared and Raman spectra of the title compound, which were acquired at room temperature, confirm the presence of three different anions (TeO_6^{6-} , SO_4^{2-} , and SeO_4^{2-}).

On the other hand, the most interesting feature in this compound consists in the presence of three phase transitions located at 411, 425 and 498 K, respectively, observed by the thermal investigation.

Acknowledgments

This work is supported by the Ministry of Higher Education and Research of Tunisia.

References

[1] A. Elferjani, S. Garcia-Granda, M. Dammak, J. Alloys Compd. 749 (2018) 448.

[2] H. Litaiem, M. Dammak, T. Mhiri, A. Cousson, J. Alloys Compd. 396 (2005) 34.

[3] L. Ktari, M. Dammak, A. Hadrich, A. Cousson, M. Nierlich, F. Romain, T. Mhiri, Solid State Sci. 6 (2004) 1393.

[4] L. Ktari, M. Dammak, A. Madani, T. Mhiri, Solid State Ion. 145 (2001) 225.

[5] H. Khemakhem, Ferroelectrics. 234 (1999) 47.

[6] R. Zilber, A. Durif, M. T. Averbuch-Pouchot, Acta Cryst. B 36 (1980) 2743.

[7] R. Zilber, A. Durif, M. T. Averbuch-Pouchot, Acta Cryst. B 37 (1981) 650.

[8] R. Zilber, A. Durif, M. T. Averbuch-Pouchot, Acta Cryst. B 38 (1982) 1554.

[9] M. Dammak, H. Khemakhem, T. Mhiri, A.W. Kolsi, A. Daoud, J. Alloys Compd. 280 (1998) 107.

[10] M. Dammak, H. Khemakhem, T. Mhiri, J. Phys. Chem. Solids. 62 (2001) 2069.

[11] M. Abdelhedi, M. Dammak, A. Cousson, M. Nierlich, A.W. Kolsi, Acta Cryst. E 61 (2005) 256.

[12] M. Abdelhedi, M. Dammak, A.W. Kolsi, A. Cousson, Analytical Sciences: X-ray Structure Analysis Online. 24 (2008) 93.

[13] L. Ktari, M. Dammak, T.Mhiri, A. W. Kolsi, Phys. Procedia. 2 (2009) 729.

[14] M. Abdelhedi, M. Dammak, A. Cousson, A.W. Kolsi, J. Alloys Compd. 398 (2005) 55.

[15] A. Elferjani, M. Abdelhedi, M. Dammak, A. W. Kolsi, J. Appl. Phys. A. 122 (2016) 742.

[16] M. Dammak, A. Hadrich, T. Mhiri, J. Alloys Compd. 428 (2007) 8.

[17] Nonius, in: B.V. Nonius (Ed.), Kappa CCD Sever Software, Delft, The Netherlands, 1999.

[18] APEX2 version 1. 0–8, Bruker AXS, Madison, WI, 2003.

[19] D. J. Watkin, C. K. Prout, J. R. Carruthers, P. W. Betteridge, R. I. Cooper, CRYSTALS Issue 11, Chemical Crystallography Laboratory, Oxford, UK, 2001.

[20] G. M. Sheldrick, SHELXS-97 and SHELXL-97, Program for Crystal Structure Refinement, Univ. of Göttingen, Germany. 1970.

[21] K. Brandenburg, M. Berndt, DIAMOND Version 2.1.b, Crystal Impact, Gb R, Bonn, Germany, 1999.

[22] M. Dammak, T. Mhiri, J. Jaud , J. M. Savariault. J. Inorg Mater. 3 (2001) 861.

[23] A. Novak, Hydrogen Bonding in Solids, Spring-Verlag, Berlin, Heidelberg, New York. 18 (1974) 177.

[24] M. Djemel, M. Abdelhedi, L. Ktari, M. Dammak, J. Mol. Struct. 1033 (2013) 84.

[25] A. Elferjani, S. Garcia-Granda, M. Dammak, J. Res. Chem. Intermed. 45 (2018) 1357.

[26] R. Ayadi, J. Lhoste, I. Ledoux-Rak, T. Mhiri, M. Boujelbene, J. Saudi Chem. Soc. 21 (2017) 869.

[27] K. Jaouadi, N. Zouari, T. Mhiri, Phase Transitions, 90 (2017) 143.

[28] N. Nouiri, K. Jaouadi, T. Mhiri N. Zouari, Ionics, 22 (2016) 1611.

[29] K. Ghorbel, H. Litaiem, L. Ktari, S. Garcia-Granda, M. Dammak, J. Mol. Struct. 1079 (2015) 225.

[30] M. Djemel, M Abdelhedi, N Zouari, M Dammak, A.W Kolsi, J. Solid State Chem. 196 (2012) 267.

Figures captions

Fig. 1. (a) Projection of crystal structure $Cs_{2.8}Tl_{1.2}$ $(SO_4)_{1.48}(SeO_4)_{0.52}.[Te(OH)_6]_2$ on the ab plane; (b) The coordination of TeO_6 groups; (c) The coordination of S/SeO_4 groups.

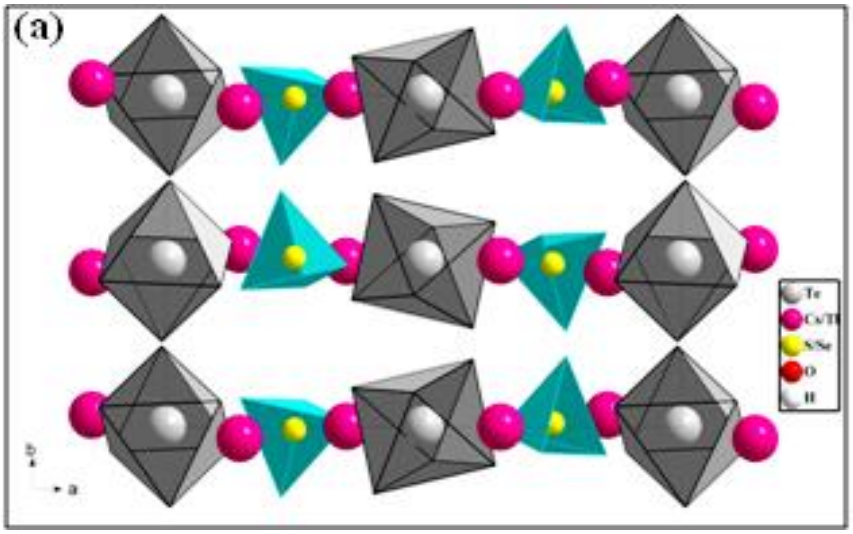

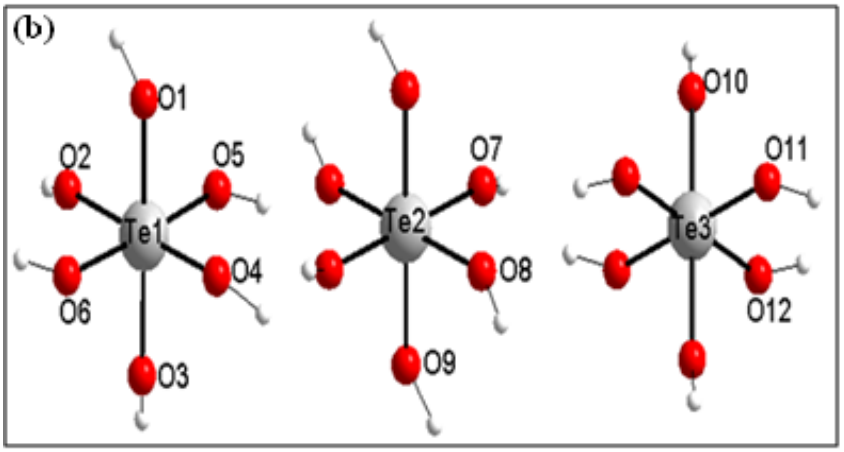

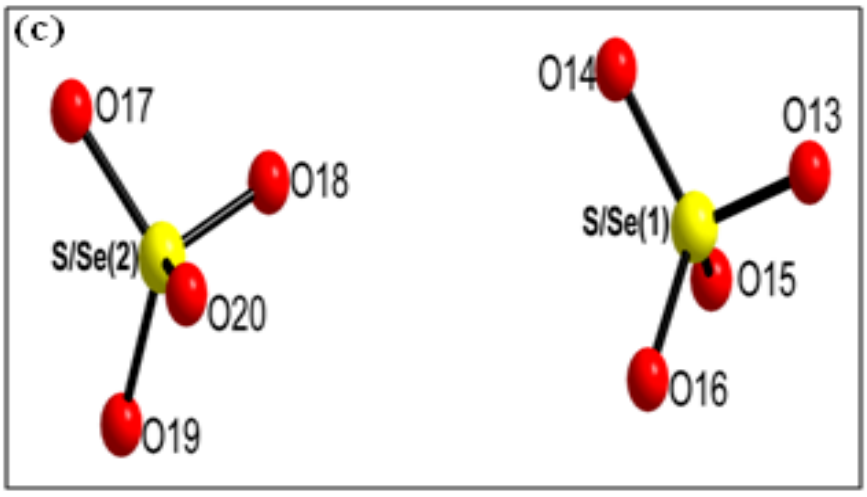

Fig. 2. Projection of the structure $Cs_{2.8}Tl_{1.2}(SO_4)_{1.48}(SeO_4)_{0.52}.[Te(OH)_6]_2$ showing the Hydrogen bonds.

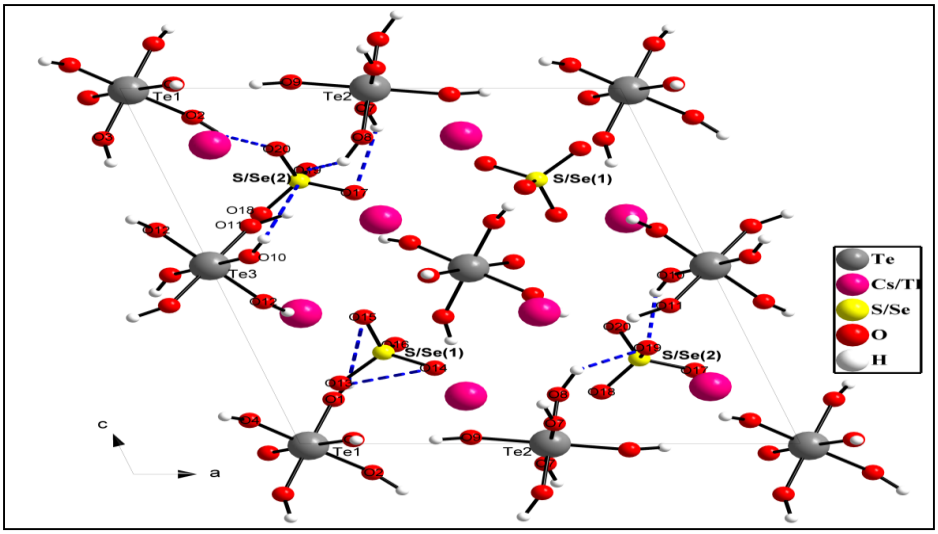

Fig. 3. Thermal analysis of $Cs_{2.8}Tl_{1.2}(SO_4)_{1.48}(SeO_4)_{0.52}.[Te(OH)_6]_2$, DSC (a), and TG–DTA (b).

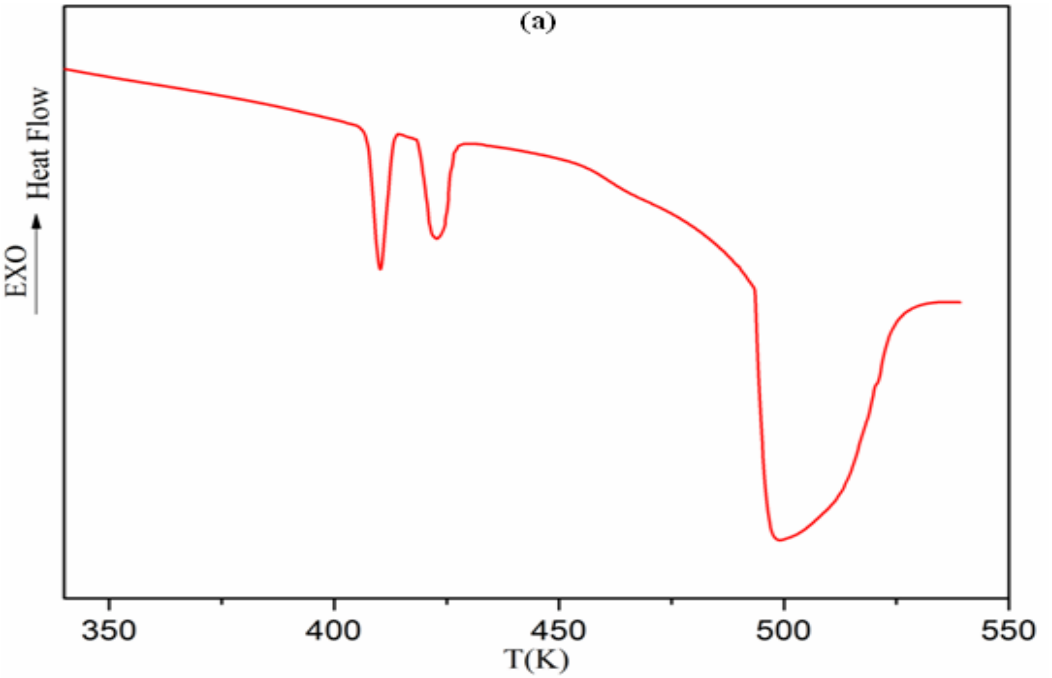

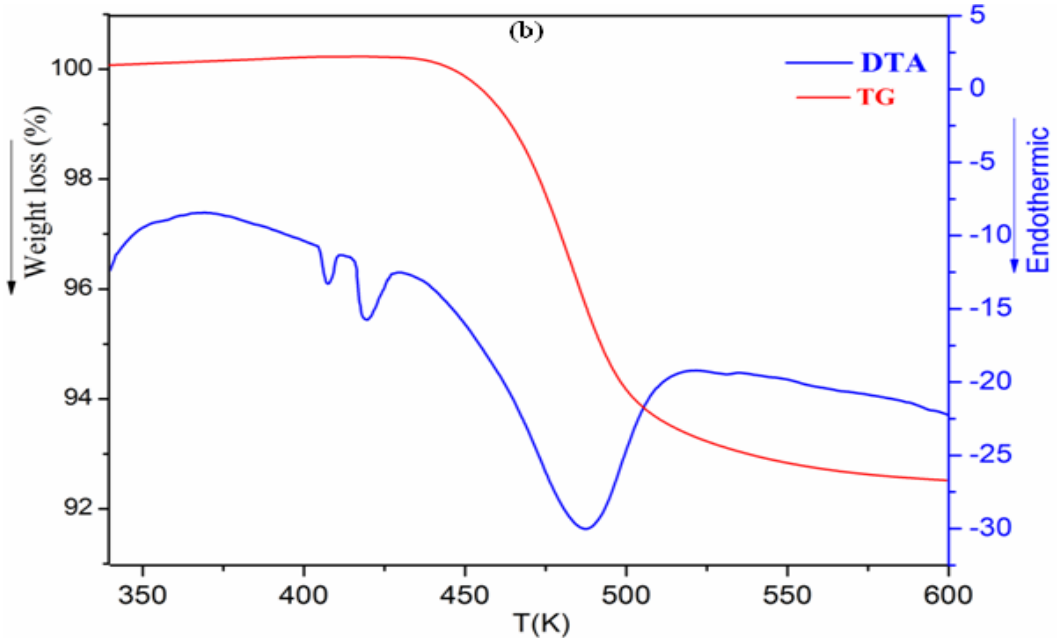
(b)
DTA
TG
Weight loss (%)
Endothermic
T(K)
100
98
96
94
92
5
0
-5
-10
-15
-20
-25
-30
350
400
450
500
550
600

Table captions

Table 1: Selected bond lengths (Å) and bond angles (°).

a- Cesium/thallium groups			
Cs/Tl(1)–O5= 2.90(1)	Cs/Tl(2)–O3=3.03(1)	Cs/Tl(3)–O6= 3.01(1)	Cs/Tl(4)–O7= 3.05(1)
Cs/Tl(1)–O19= 2.93(1)	Cs/Tl(2)–O10= 3.09(1)	Cs/Tl(3)–O8= 3.04(1)	Cs/Tl(4)–O14= 3.10(1)
Cs/Tl(1)–O9= 2.932(8)	Cs/Tl(2)–O16= 3.10(1)	Cs/Tl(3)–O2= 3.05(1)	Cs/Tl(4)–O1= 3.14(1)
Cs/Tl(1)–O4= 3.00(1)	Cs/Tl(2)–O1= 3.23(1)	Cs/Tl(3)–O17= 3.12(1)	Cs/Tl(4)–O12= 3.21(1)
Cs/Tl(1)–O13= 3.09(1)	Cs/Tl(2)–O18= 3.23(1)	Cs/Tl(3)–O11= 3.18(1)	Cs/Tl(4)–O16= 3.25(1)
Cs/Tl(1)–O11= 3.10(1)	Cs/Tl(2)–O8= 3.38(1)	Cs/Tl(3)–O14= 3.221(9)	Cs/Tl(4)–O17= 3.270(9)
Cs/Tl(1)–O20= 3.12(1)	Cs/Tl(2)–O7= 3.41(1)		Cs/Tl(4)–O3= 3.49(1)
Cs/Tl(1)–O12= 3.276(9)	Cs/Tl(2)–O5= 3.439(9)		
b- Sulfate/selenate groups			
S/Se(1)–O13= 1.496 (9)	O13–S/Se(1)–O14= 105.9 (6)		O17–S/Se(2)–O18= 108.5 (6)
S/Se(1)–O14= 1.495 (1)	O13–S/Se(1)–O15= 111.4 (4)		O17–S/Se(2)–O19= 106.8 (6)
S/Se(1)–O15= 1.488 (1)	O14–S/Se(1)–O15= 110.8 (6)		O18–S/Se(2)–O19= 108.6 (6)
S/Se(1)–O16= 1.471 (1)	O13–S/Se(1)–O16= 107.9 (6)		O17–S/Se(2)–O20= 109.5 (6)
	O14–S/Se(1)–O16=110.1 (6)		O18–S/Se(2)–O20= 110.9 (5)
S/Se(2)–O17= 1.466 (1)	O15–S/Se(1)–O16= 110.5 (6)		O19–S/Se(2)–O20= 112.5 (6)
S/Se(2)–O18= 1.472 (9)			
S/Se(2)–O19= 1.506 (1)			
S/Se(2)–O20= 1.494 (1)			
c- Tellurate groups			
Te(1)–O1= 1.862 (9)	O1–Te(1)–O2= 91.0 (4)		O3–Te(1)–O5= 89.2 (4)
Te(1)–O2= 1.962 (1)	O1–Te(1)–O3= 178.9 (5)		O4–Te(1)–O5= 91.2 (5)
Te(1)–O3= 1.923 (9)	O2–Te(1)–O3= 88.0 (4)		O1–Te(1)–O6= 88.2 (4)
Te(1)–O4= 1.828 (1)	O1–Te(1)–O4= 88.6 (4)		O2–Te(1)–O6= 88.4 (4)
Te(1)–O5= 1.926 (1)	O2–Te(1)–O4= 178.9 (4)		O3–Te(1)–O6= 91.2 (4)

Te(1)–O6= 1.901 (1)	O3–Te(1)–O4= 92.4 (4)	O4–Te(1)–O6= 92.7 (5)
	O1–Te(1)–O5= 91.3 (4)	O5–Te(1)–O6=176.1 (5)
	O2–Te(1)–O5= 87.8 (4)	
Te(2)–O9(i)= 1.896 (1)	O9(i)–Te(2)–O8(i)= 90.3 (4)	O7(i)–Te(2)–O8= 90.7 (4)
Te(2)–O8(i)= 1.874 (1)	O9(i)–Te(2)–O7(i)= 90.5 (5)	O7–Te(2)–O8= 89.3 (4)
Te(2)–O7(i)= 1.871 (1)	O8(i)–Te(2)–O7(i)= 89.3 (4)	O9(i)–Te(2)–O9= 180
Te(2)–O7= 1.871 (1)	O9(i)–Te(2)–O7= 89.5 (5)	O8(i)–Te(2)–O9= 89.7 (4)
Te(2)–O8= 1.874(1)	O8(i)–Te(2)–O7=90.7 (4)	O7(i)–Te(2)–O9= 89.5 (5)
Te(2)–O9= 1.896 (1)	O7(i)–Te(2)–O7= 180	O7–Te(2)–O9= 90.5 (5)
	O9(i)–Te(2)–O8= 89.7 (4)	O8–Te(2)–O9= 90.3 (4)
	O8(i)–Te(2)–O8= 180	
Te(3)–O10(ii)= 1.919 (1)	O10(ii)–Te(3)–O11(ii)= 90.4 (4)	O12(ii)–Te(3)–O11= 92.0 (5)
Te(3)–O11(ii)= 1.878 (9)	O10(ii)–Te(3)–O12(ii)= 89.8 (5)	O10–Te(3)–O11= 90.4 (4)
Te(3)–O12(ii)= 1.848 (1)	O11(ii)–Te(3)–O12(ii)= 88.0 (5)	O10(ii)–Te(3)–O12= 90.2(5)
Te(3)–O10= 1.919 (1)	O10(ii)–Te(3)–O10= 180	O11(ii)–Te(3)–O12= 92.0 (5)
Te(3)–O11= 1.878 (9)	O11(ii)–Te(3)–O10= 89.6 (4)	O12(ii)–Te(3)–O12= 180
Te(3)–O12= 1.848(1)	O12(ii)–Te(3)–O10= 90.2 (5)	O10–Te(3)–O12= 89.8 (5)
	O10(ii)–Te(3)–O11= 89.6 (4)	O11–Te(3)–O12= 88.0 (5)
	O11(ii)–Te(3)–O11= 180	

Symmetry codes: (i) $-x+2, -y+1, -z+1$; (ii) $-x+2, -y, -z+1$.

Table 2: Hydrogen-bond and short contact geometry (Å, °).

D—H…A	D—H	H…A	D…A	D—H…A
O_1–H_1…O_{14}^{iii}	0.970	2.296	3.139(4)	144.9 (7)
O_1–H_1…O_{15}^{iii}	0.970	2.002	2.800(4)	138.2 (7)
O_2–H_2…O_{20}	0.954	1.979	2.732(4)	134.2 (7)
O_7–H_7…O_{17}	0.966	2.428	3.225(5)	139.6 (6)
O_8–H_8…O_{19}^{iv}	0.960	2.315	3.022(4)	129.9 (7)
O_{10}–H_{10}…O_{19}^{ii}	0.959	1.951	2.646(4)	127.5 (7)

Symmetry codes : (ii) $-x+2, -y, -z+1$; (iii) $-x+3/2, y-1/2, -z+3/2$; (iv) $x+1/2, -y+1/2, z+1/2$.

Table 3: Observed IR and Raman frequencies (cm^{-1}) and band assignments for $Cs_{2.8}Tl_{1.2}(SO_4)_{1.48}(SeO_4)_{0.52}.[Te(OH)_6]_2$ at room temperature.

IR	***I***	***Raman***	***I***	***Assignment***
-		60	w	T(Tl^+)
-		119	w	T(S/SeO_4^{2-} ; TeO_6^{6-})
-		184	vw	υ(OH…O)
-		319	m	$\upsilon_2(SeO_4)$
-		356	w	$\upsilon_4(TeO_6)$
-		362	m	$\upsilon_5(TeO_6)$
-		412	s	$\upsilon_4(SeO_4)$
-		437	vw	$\upsilon_4(SeO_4)$
471		475	w	$\upsilon_2(SO_4)$ and $\upsilon_2(SeO_4)$
596	s	-		$\upsilon_3(TeO_6)$
673	vs	650	vs	$\upsilon_1(TeO_6)$
-		831	m	$\upsilon_1(SeO_4)$
865	s	-		$\upsilon_3(SeO_4)$
-		969	s	$\upsilon_1(SO_4)$
1077	vs	-		$\upsilon_3(SO_4)$
1481	m	-		

2327	s	-	υ(OH) of hydrogen
2365	s	-	bonds
3058	vs	-	υ(OH) of $Te(OH)_6$

Relative intensities: vs: very strong; s: strong; m: medium; w: weak; vw: very weak.

Supporting Information:

Table S1. Main crystallographic, feature X-ray diffraction data parameters results of $Cs_{2.8}Tl_{1.2}(SO_4)_{1.48}(SeO_4)_{0.52}.[Te(OH)_6]_2$.

Formula	$Cs_{2.80}Tl_{1.20}(SO_4)_{1.48}(SeO_4)_{0.52}[Te(OH)_6]$
Formula weight ($gmol^{-1}$)	1292.72
T (K)	293
Crystal system	Monoclinic
Space group	$P2_1/n$
Unit cell dimensions	a= 11.8967(4) Å b= 14.1486(5) Å c= 13.1612(5) Å β = 108.973(1)° V = 2094.96(13) $Å^3$
Z	4
Dx ($g.cm^{-3}$)	4.098(4)
θ range for data collection (°)	2.8-26.8
μ (mm^{-1})	17.89
hkl range	$-15 \leq h \leq 15$ $-17 \leq k \leq 17$ $-16 \leq l \leq 16$
Data collection instrument	Kappa CCD
Wavelength (Å)	0.71073
Measured reflections	104174
Observed reflections $I>2\sigma(I)$	1568
R indices	R=0.056 and R_w=0.105
Goodness-of-fit on (F^2)	1.00
$w = 1/[\sigma^2 (Fo^2)+(0.0800P)^2 +0P]$ where $P = (Fo^2+2Fc^2)/3$	
CCDC deposition number	1909846

Table S2. Atomic coordinates and equivalent thermal parameters.

Atoms	X	Y	Z	U_{eq}	Occupation
Te1	0.51482(17)	0.26197(11)	0.49371(16)	0.0335(5)	1.0000
Te2	1.0000	0.5000	0.5000	0.0285(5)	0.5000
Te3	1.0000	0.0000	0.5000	0.0302(5)	0.5000
Cs1	0.62227(6)	0.49987(6)	0.33995(6)	0.0520(4)	0.09923(3)
Tl1	0.62227(6)	0.49987(6)	0.33995(6)	0.0520(4)	0.89923(3)
Cs2	0.87987(8)	0.26565(8)	0.63340(8)	0.0441(4)	0.90011(6)
Tl2	0.87987(8)	0.26565(8)	0.63340(8)	0.0441(4)	0.10011(6)
Cs3	0.61195(7)	–0.00641(7)	0.37021(7)	0.0387(4)	0.89983(8)
Tl3	0.61195(7)	–0.00641(7)	0.37021(7)	0.0387(4)	0.09983(8)
Cs4	0.63366(8)	0.25012(8)	0.86607(8)	0.0489(5)	0.89991(7)
Tl4	0.63366(8)	0.25012(8)	0.86607(8)	0.0489(4)	0.09991(7)
S1	0.75940(2)	0.49854(2)	0.75673(2)	0.0117(4)	0.75734(7)
Se1	0.75940(2)	0.49854(2)	0.75673(2)	0.0117(4)	0.23734(7)
S2	0.76412(3)	0.25190(3)	0.23866(3)	0.0128(4)	0.72127(2)
Se2	0.76412(3)	0.25190(3)	0.23866(3)	0.0128(4)	0.28127(2)
O1	0.6122(8)	0.2141(8)	0.6245(8)	0.0529(5)	1.0000
O2	0.6158(8)	0.2049(8)	0.4184(8)	0.0563(5)	1.0000
O3	0.4151(8)	0.3094(8)	0.3573(8)	0.0562(5)	1.0000
O4	0.4230(8)	0.3168(8)	0.5651(8)	0.0535(5)	1.0000
O5	0.6110(8)	0.3741(7)	0.5112(8)	0.0439(5)	1.0000
O6	0.4273(8)	0.1471(7)	0.4729(8)	0.0483(5)	1.0000
O7	0.9706(8)	0.3777(8)	0.4435(8)	0.0637(5)	1.0000
O8	1.0655(8)	0.4483(8)	0.6378(8)	0.0587(5)	1.0000
O9	0.8480(8)	0.5033(8)	0.5174(8)	0.0566(5)	1.0000
O10	1.0887(8)	–0.1158(7)	0.5261(8)	0.0529(5)	1.0000
O11	0.8787(8)	–0.0575(8)	0.3883(8)	0.0997(5)	1.0000
O12	1.0708(8)	0.0338(8)	0.3994(8)	0.0959(5)	1.0000

O13	0.6414(8)	0.5032(8)	0.6698(8)	0.0709(5)	1.0000
O14	0.8458(8)	0.5456(8)	0.7123(8)	0.0595(5)	1.0000
O15	0.7561(8)	0.5471(8)	0.8560(8)	0.0441(5)	1.0000
O16	0.7907(8)	0.3982(7)	0.7786(8)	0.0733(5)	1.0000
O17	0.8629(8)	0.2880(8)	0.2062(8)	0.0604(5)	1.0000
O18	0.6549(8)	0.2560(8)	0.1452(8)	0.0637(5)	1.0000
O19	0.7915(8)	0.1499(7)	0.2696(8)	0.0717(5)	1.0000
O20	0.7520(8)	0.3102(8)	0.3291(8)	0.0393(5)	1.0000
H1	0.6562	0.1617	06665	0.0635	1.0000
H2	0.6571	0.2098	0.3675	0.0685	1.0000
H3	0.4067	0.3410	0.2900	0.0671	1.0000
H4	0.3774	0.3708	0.5759	0.0639	1.0000
H5	0.6159	0.4417	0.5092	0.0527	1.0000
H6	0.4257	0.0790	0.4757	0.0564	1.0000
H7	0.9741	0.3325	0.3896	0.0751	1.0000
H8	1.1273	0.4477	0.7063	0.0688	1.0000
H9	0.7754	0.5373	0.5106	0.0692	1.0000
H10	1.1356	–0.1619	0.5752	0.0634	1.0000
H11	0.7936	–0.0692	0.3537	0.1197	1.0000
H12	1.1086	0.0827	0.3696	0.1137	1.0000

$U_{eq} = 1/3 \sum_i \sum_j U_{ij}\, a_i^* a_j^* a_i a_j$

Table S3. Anisotropic displacement parameters of $Cs_{2.8}Tl_{1.2}(SO_4)_{1.48}(SeO_4)_{0.52}.[Te(OH)_6]_2$ compound.

Atoms	U^{11}	U^{22}	U^{33}	U^{12}	U^{13}	U^{23}
Te1	0.0395 (5)	0.0291 (6)	0.0302 (5)	0.0043 (6)	0.0089 (5)	0.0040 (6)
Te2	0.02558 (7)	0.02964 (7)	0.02819 (7)	−0.00180 (7)	0.00596 (7)	−0.00429 (7)
Te3	0.03022 (7)	0.03073 (7)	0.02805 (7)	−0.00351 (7)	0.00734 (7)	−0.00339 (7)
Cs1	0.05238 (6)	0.04951 (6)	0.05235 (6)	−0.00039 (6)	0.01472 (6)	0.00281 (6)
Tl1	0.05238 (6)	0.04951 (6)	0.05235 (6)	−0.00039 (6)	0.01472 (6)	0.00281 (6)
Cs2	0.04085 (8)	0.04841 (8)	0.04496 (8)	0.00203 (8)	0.01672 (8)	−0.00332 (8)
Tl2	0.04085 (8)	0.04841 (8)	0.04496 (8)	0.00203 (8)	0.01672 (8)	−0.00332 (8)
Cs3	0.03975 (7)	0.03830 (7)	0.03880 (7)	0.00473 (7)	0.01387 (7)	0.00455 (7)
Tl3	0.03975 (7)	0.03830 (7)	0.03880 (7)	0.00473 (7)	0.01387 (7)	0.00455 (7)
Cs4	0.04502 (8)	0.04444 (8)	0.06310 (8)	−0.00422 (8)	0.02569 (8)	−0.00154 (8)
Tl4	0.04502 (8)	0.04444 (8)	0.06310 (8)	−0.00422 (8)	0.02569 (8)	−0.00154 (8)
S1	0.01241 (12)	0.01268 (12)	0.01260 (12)	−0.00019 (12)	0.00780 (12)	0.00066 (12)
Se1	0.01241 (12)	0.01268 (12)	0.01260 (12)	−0.00019 (12)	0.00780 (12)	0.00066 (12)
S2	0.01039 (13)	0.01159 (13)	0.01676 (13)	0.00388 (13)	0.00479 (13)	−0.00203 (13)
Se2	0.01039 (13)	0.01159 (13)	0.01676 (13)	0.00388 (13)	0.00479 (13)	−0.00203 (13)
O1	0.0621 (6)	0.0448 (9)	0.0470 (9)	−0.0056 (9)	0.0111 (9)	0.0014 (9)
O2	0.0619 (6)	0.0623 (9)	0.0641 (9)	0.0000 (9)	0.0474 (9)	0.0015 (9)
O3	0.0622 (6)	0.0459 (9)	0.0559 (9)	−0.0153 (9)	0.0129 (9)	−0.0001 (9)
O4	0.0551 (6)	0.0555 (9)	0.0606 (9)	0.0055 (9)	0.0334 (9)	0.0103 (9)
O5	0.0423 (6)	0.0411 (9)	0.0522 (9)	−0.0210 (9)	0.0206 (9)	0.0016 (9)
O6	0.0578 (6)	0.0382 (9)	0.0540 (9)	−0.0082 (9)	0.0253 (9)	−0.0040 (9)
O7	0.0599 (6)	0.0555 (9)	0.0710 (9)	0.0117 (9)	0.0149 (9)	−0.0194 (9)
O8	0.0660 (6)	0.0699 (9)	0.0527 (9)	0.0046 (9)	0.0363 (9)	0.0033 (9)
O9	0.0389 (6)	0.0816 (9)	0.0559 (9)	0.0050 (9)	0.0244 (9)	−0.0092 (9)
O10	0.0599 (6)	0.0422 (9)	0.0579 (9)	0.0154 (9)	00210 (9)	−0.0046 (9)

O11	0.0908 (6)	0.0615 (9)	0.1032 (9)	−0.0053 (9)	−0.0286 (9)	−0.0102 (9)
O12	0.1042 (6)	0.1060 (9)	0.1011 (9)	0.0333 (9)	0.0659 (9)	0.0320 (9)
O13	0.0636 (6)	0.0706 (9)	0.0645 (9)	0.0050 (9)	0.0017 (9)	−0.0159 (9)
O14	0.0709 (6)	0.0669 (9)	0.0618 (9)	−0.0221 (9)	0.0508 (9)	−0.0139 (9)
O15	0.0566 (6)	0.0365 (9)	0.0511 (9)	−0.0031 (9)	0.0339 (9)	−0.0110 (9)
O16	0.0820 (6)	0.0647 (9)	0.0594 (9)	0.0134 (9)	0.0042 (9)	0.0035 (9)
O17	0.0515 (6)	0.0833 (9)	0.0550 (9)	−0.0098 (9)	0.0289 (9)	−0.0068 (9)
O18	0.0431 (6)	0.0726 (9)	0.0742 (9)	0.0073 (9)	0.0176 (9)	−0.0111 (9)
O19	0.0828 (6)	0.0565 (9)	0.0687 (9)	0.0012 (9)	0.0150 (9)	0.0002 (9)
O20	0.0506 (6)	0.0181 (9)	0.0559 (9)	−0.0019 (9)	0.0265 (9)	−0.0051 (9)

The anisotropic displacement exponent takes the form: $\exp[-2\pi^2 \sum_i \sum_j Uij\ h_i h_j\ a_i a_j^*\ ]$

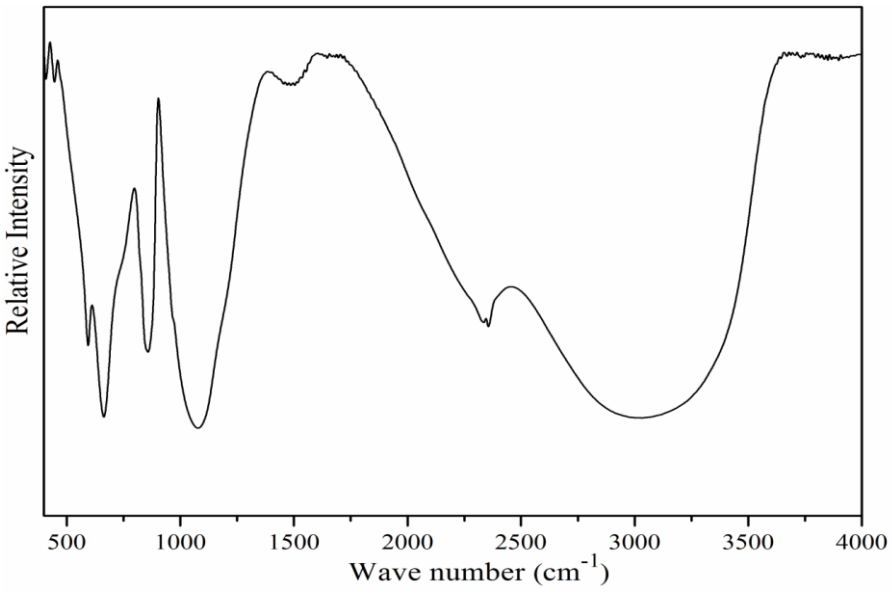

Fig. S1. IR spectrum at room temperature of $Cs_{2.8}Tl_{1.2}(SO_4)_{1.48}(SeO_4)_{0.52}.[Te(OH)_6]_2$ compound.

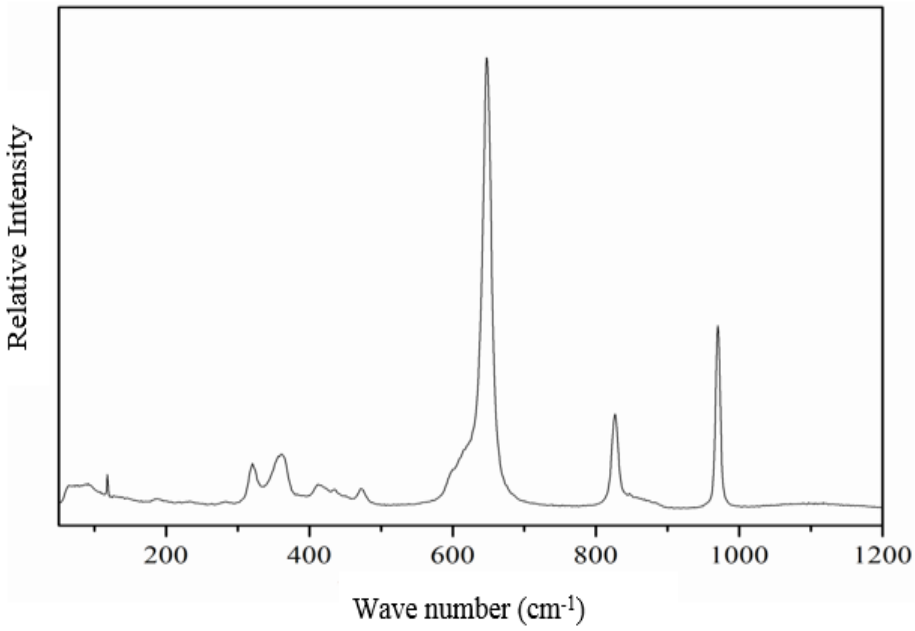

Fig. S2. Raman spectra at room temperature of $Cs_{2.8}Tl_{1.2}(SO_4)_{1.48}(SeO_4)_{0.52}.[Te(OH)_6]_2$ compound.